

Artificial Photosyntheses: Single-Chain Nanoparticles with Manifold Visible-Light Photocatalytic Activity for Challenging “in Water” Organic Reactions

Davide Arena,* Ester Verde-Sesto, Iván Rivilla, and José A. Pomposo*



Cite This: *J. Am. Chem. Soc.* 2024, 146, 14397–14403



Read Online

ACCESS |

Metrics & More

Article Recommendations

Supporting Information

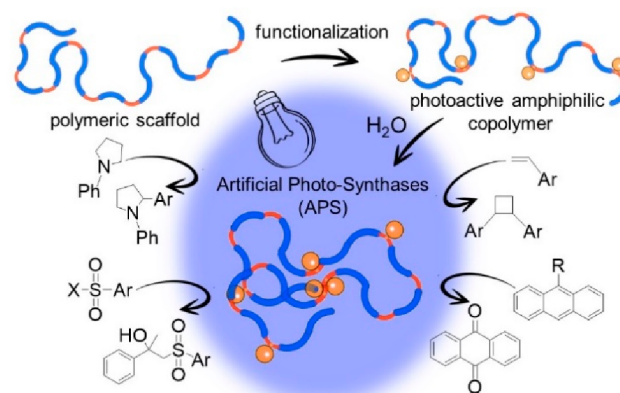
ABSTRACT: Photocatalyzed reactions of organic substances in aqueous media are challenging transformations, often because of scarce solubility of substrates and catalyst deactivation. Herein, we report single-chain nanoparticles, SCNPs, capable of efficiently catalyzing four different “in water” organic reactions by employing visible light as the only external energy source. Specifically, we decorated a high-molecular-weight copolymer, poly(OEGMA_{300-r}-AEMA), with iridium(III) cyclometalated complex pendants at varying content amounts. The isolated functionalized copolymers demonstrated self-assembly into noncovalent, amphiphilic SCNPs in water, which enabled efficient visible-light photocatalysis of two reactions unprecedentedly reported in water, namely, [2 + 2] photocycloaddition of vinyl arenes and α -arylation of *N*-arylamines. Additionally, aerobic oxidation of 9-substituted anthracenes and β -sulfonylation of α -methylstyrene were successfully carried out in aqueous media. Hence, by merging metal-mediated photocatalysis and SCNPs for the fabrication of artificial photoenzyme-like nano-objects—i.e., artificial photosyntheses (APS)—our work broadens the possibilities for performing challenging “in water” organic transformations via visible-light photocatalysis.

In nature, only three types of enzymes carry out purely photocatalytic organic reactions.^{1–3} Indeed, the design of abiotic protein nanoreactors capable of custom photoreactions requires extensive genetic engineering effort.^{4–6} In organic photochemistry, the scarce solubility of reactants in aqueous media and severe catalyst deactivation are of central concern for the replacement of organic solvents with water. While several strategies have been recently proposed,^{7–10} only a few works have been devoted to the use of ultrafine soft nano-objects as efficient visible-light photocatalysts of “in water” organic reactions.^{11,12}

Single-chain nanoparticles (SCNPs)—as intramolecularly self-folded synthetic polymer chains with ultrasmall size (2–20 nm)—are posed as perfect candidates for advanced, next-generation enzyme-mimetic catalyst preparation.^{13–16} Despite the extensive use of SCNPs as nanoreactors for a plethora of organic reactions,^{13–19} only a few works have disclosed the use of SCNPs for photocatalytic applications.^{12,20} Herein, we report the construction of unimolecular soft nano-objects endowed with broad, manifold photocatalytic activity in water and constructed by taking advantage of the protein-mimetic architecture of polymeric SCNPs (see Scheme 1). These artificial photosyntheses (APS) are used to perform a collection of four visible-light-induced transformations using water as the sole medium.

As APS precursor, we prepared the polymeric scaffold poly(OEGMA_{300-r}-AEMA) P1 of high molecular weight (>150 kDa), low dispersity (1.06), and controlled chemical composition (Table 1) via reversible addition–fragmentation chain transfer (RAFT) copolymerization of the monomers 4-acetoacetoxyethyl methacrylate (AEMA) and (oligoethylene glycol monomethyl ether) methacrylate (OEGMA₃₀₀). To

Scheme 1. Illustration of the Preparation of an Artificial Photosynthese (APS) Endowed with Manifold Photocatalytic Activity toward “in Water” Reactions



endow P₁ with photocatalytic activity, we exploited the β -ketoester reactivity provided by the hydrophobic AEMA groups. We prepared iridium (Ir)(III)-containing copolymers at three loading (L^{Ir}) regimes, P₁-Ir₁₀, P₁-Ir₂₃, and P₁-Ir₄₀ (L^{Ir} = 10, 23, and 40 mol % with respect to AEMA units, respectively), by decorating the copolymer P₁ through reaction

Received: February 23, 2024

Revised: April 15, 2024

Accepted: April 16, 2024

Published: April 19, 2024

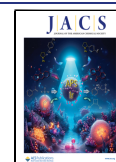
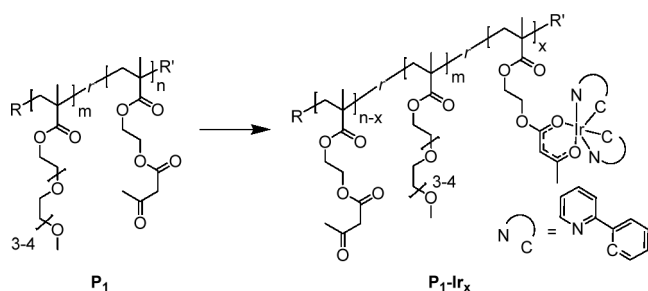


Table 1. Properties of Neat (P_1) and Functionalized Copolymers (P_1 -Ir $_x$) Synthesized in This Work

sample	M_w (kDa) ^a	D^b	AEMA (mol %) ^c	L^r (mol %) ^d
P_1	169.8	1.06	20	
P_1 -Ir ₁₀	178.6	1.10	18	10
P_1 -Ir ₂₃	174.5	1.13	15.4	23
P_1 -Ir ₄₀	211.7	1.03	12	40

^aWeight-average molecular weight. ^bDispersity. ^cMolar content of AEMA units. ^dIridium content (see the SI).

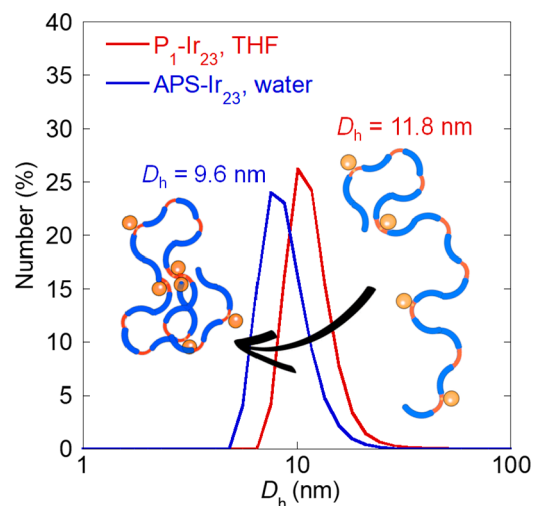
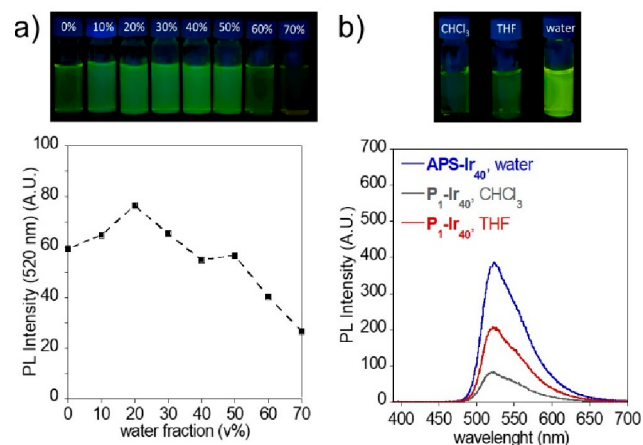
with the dihydroxotetrakis[2-(2-pyridinyl)phenyl]diiridium(III) dimer $[\text{Ir}(\text{ppy})_2\text{OH}]_2$ C_1 under mild conditions [see the Supporting Information (SI)].²¹

Thanks to their amphiphilic nature, high molecular weight (>150 kDa), and finely tuned composition, stable, self-assembled SCNPs^{22,23} that we denoted as SCNP- P_1 , APS-Ir₁₀, APS-Ir₂₃, and APS-Ir₄₀ were obtained upon simple dissolution of P_1 , P_1 -Ir₁₀, P_1 -Ir₂₃, and P_1 -Ir₄₀, respectively, in water. Self-assembly was ascertained by measuring via dynamic light scattering (DLS) the difference ΔD_h between hydrodynamic diameters D_h of P_1 , P_1 -Ir₁₀, P_1 -Ir₂₃, and P_1 -Ir₄₀ in tetrahydrofuran, THF, (good solvent for AEMA and OEGMA₃₀₀) and those of SCNP- P_1 , APS-Ir₁₀, APS-Ir₂₃, and APS-Ir₄₀ measured in water (selective solvent for OEGMA₃₀₀). Iridium-functionalized copolymers all presented a positive ΔD_h (Table 2) because of the formation of a self-collapsed architecture (see Figure 1 and the SI).

Table 2. Hydrodynamic Radii Measured in THF (Good Solvent) and Water (Selective Solvent)

sample	D_h (THF) (nm)	sample	D_h (water) (nm)
P_1	9.9	SCNP- P_1	8.7
P_1 -Ir ₁₀	12.3	APS-Ir ₁₀	10.4
P_1 -Ir ₂₃	11.8	APS-Ir ₂₃	9.6
P_1 -Ir ₄₀	10.4	APS-Ir ₄₀	9.1

Additional evidence of the formation of a self-assembled conformation in APS-Ir₁₀, APS-Ir₂₃, and APS-Ir₄₀ was obtained through photoluminescence (PL) experiments. As illustrated in Figure 2a, we measured the PL of eight solutions of a model compound, bis(2-phenylpyridine)(methyl acetoacetonate)iridium(III) C_2 (see the SI), in THF/water mixtures upon increase of the water content (from 0% to 70%). We observed a decrease in the PL intensity of C_2 at high water content, which is consistent with literature data reported for the analogous complex bis(2-phenylpyridine)-(acetylacetonate)iridium(III), Ir(ppy)₂(acac).^{24,25} Conversely, APS-Ir₁₀, APS-Ir₂₃, and APS-Ir₄₀ in water displayed significant PL intensity enhancement with respect to P_1 -Ir₁₀, P_1 -Ir₂₃, and P_1 -Ir₄₀ recorded in two different nonselective solvents (chloroform and THF) (see Figure 2b). This finding suggests

**Figure 1.** Illustration of the reduction in hydrodynamic size due to self-assembly of P_1 -Ir₂₃ (linear architecture) to APS-Ir₂₃ (SCNP architecture) upon change from THF (good solvent) to water (selective solvent).**Figure 2.** (a) PL emission of model compound bis(2-phenylpyridine)(methyl acetoacetonate)iridium(III) C_2 in THF/water mixtures (from 0% to 70%) ($[\text{Ir}(\text{III})] = 3 \mu\text{M}$, $\lambda_{\text{exc}} = 450 \text{ nm}$). (b) Illustration of the aggregation-enhanced emission (AEE) of APS-Ir₄₀ in water vs P_1 -Ir₄₀ in CHCl_3 and THF under LED illumination ($[\text{Ir}(\text{III})] = 3 \mu\text{M}$, $\lambda_{\text{exc}} = 450 \text{ nm}$, $\lambda_{\text{em}}(\text{max}) = 521 \text{ nm}$).

that confinement of the hydrophobic photocatalyst in the limited space of the self-assembled APS-Ir₁₀, APS-Ir₂₃, and APS-Ir₄₀ induces significant aggregation-enhanced emission (AEE).

With the self-assembled SCNPs in hand, we tested their suitability as artificial photosyntheses (APS) for in water photocatalysis of a variety of organic transformations, which were selected from among the plethora of iridium(III) cyclometalated complex-mediated reactions in organic solvents.^{26–28}

Visible light has been recently applied successfully as an energy source for [2 + 2] cycloadditions in organic solvents;²⁹ herein, we report an unprecedented procedure that employs water as the sole reaction medium. For instance, an APS-Ir₄₀ solution was prepared by dissolving 2 mg of P_1 -Ir₄₀ in 1 mL of deionized water, which was then charged with 58 μmol of the vinylic compound **1a**, and the resulting mixture was left stirring at room temperature and under LED illumination ($\lambda_{\text{max}} = 450$

nm) for 12 h. After this time, the extracted crude product was analyzed via quantitative ^1H NMR (see the SI) for conversion (c%) determination. Multiplets at 3.54 and 3.98 ppm (see Figure 3) indicate the formation of the 1,2-bis-substituted

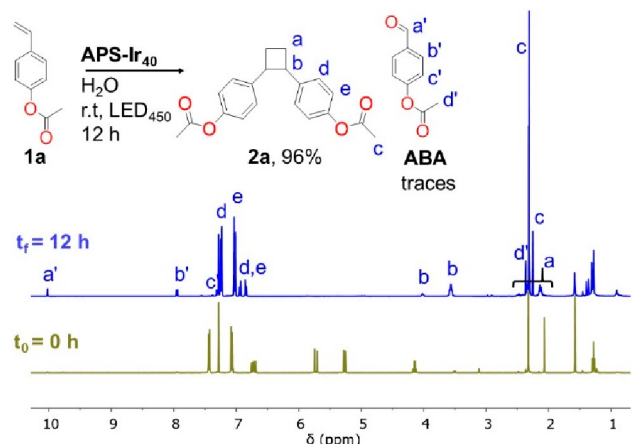
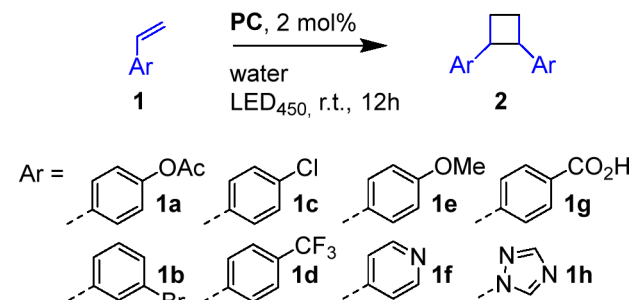


Figure 3. ^1H NMR of the crude of “in water” [2 + 2] photocycloaddition reaction of **1a** in the presence of APS-Ir₄₀ (see the text).

cyclobutane product **2a**, which was then isolated in 90% yield as a mixture of cis and trans diastereomers. To our delight, we observed similar results when exploring a variety of substrates, as illustrated in Table 3.

Considering typical redox potentials of vinyl arenes (e.g., $E_{\text{ox}} = 1.97$ V vs SCE, $E_{\text{red}} = -2.53$ V vs SCE)^{30,31} and photocatalyst excited-state potentials (e.g., $E_{\text{ox}}^* = 0.43$ V vs

Table 3. Photocatalyzed “in Water” [2 + 2] Cycloaddition of Vinyl Arenes (CA Reaction)^a



entry	photocatalyst (PC)	transformation	c% ^b	trans/cis ^c
1	APS-Ir ₄₀	1a → 2a	96(90) ^d	1:0.3
2	APS-Ir ₂₃	1a → 2a	94	1:0.3
3	APS-Ir ₁₀	1a → 2a	96	1:0.3
4	APS-Ir ₄₀	1b → 2b	97	1:0.2
5	APS-Ir ₄₀	1c → 2c	96	1:0.3
6	APS-Ir ₄₀	1d → 2d	90	1:0.3
7	APS-Ir ₄₀	1e → 2e	60	1:0.3
8	APS-Ir ₄₀	1f → 2f	79	1:0.3
9	APS-Ir ₄₀	1g → 2g	n.p. ^e	
10	APS-Ir ₄₀	1h → 2h	n.p. ^e	
11	no PC	1a → 2a	n.p. ^e	
12	C ₂	1a → 2a	63	1:0.3

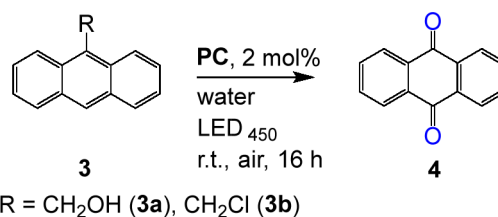
^aSee SI for experimental details. ^bConversion from ^1H NMR. ^cDetermined by ^1H NMR. ^dIsolated yield in parentheses. ^eNo product.

SCE and $E_{\text{red}}^* = -2.57$ V vs SCE),²⁶ it seems difficult to imagine the activation of olefins **1a–1f** by typical single-electron transfer (SET).³² We hypothesized that, helped by the locally hydrophobic packed environment of the APS, these unlike processes could be allowed via an energy transfer (E_{T}) mechanism because of the similar triplet energies of the involved species (e.g., $E_{\text{T}} = \sim 60$ kcal mol⁻¹ for vinyl arenes, $E_{\text{T}} = \sim 55$ kcal mol⁻¹ for C₂).³³

Byproducts formed in trace amounts, among which we assigned³⁴ the structure of 4-acetoxybenzaldehyde, ABA, to be the major constituent in agreement with the reactivity of electron-rich vinyl arenes with reactive oxygen species that may be generated during irradiation.³⁵ Performance of the same reaction using the model photocatalyst C₂ dropped conversion to 63% (see the SI) with the remaining components of the crude being the reactant and byproducts. No conversion was observed by employing water-soluble substrates (**1g**, **1h**, Table 3), probably because of differences in the E_{T} values.

Interestingly, when 9-substituted anthracenes were employed as the substrate, we observed the formation of anthraquinone **4**. Since singlet oxygen and other reactive oxygen species (ROS) are generated upon excitation of C₂ in organic solvents under aerobic conditions,³⁶ we surmised that APS-Ir₁₀, APS-Ir₂₃, and APS-Ir₄₀ could be efficient photocatalysts for the “in water” oxidation of 9-substituted anthracenes **3** to anthraquinone **4** via reaction with ROS species³⁷ (see Table 4). The formation of **4** that was confirmed

Table 4. Photocatalyzed “in Water” Oxidation of 9-Substituted Anthracenes (OA Reaction)^a

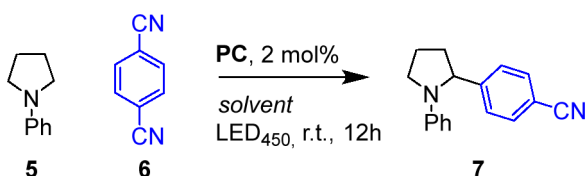


entry	photocatalyst (PC)	substrate	c% ^b
1	APS-Ir ₄₀	3a	62(58) ^c
2	APS-Ir ₂₃	3a	21
3	APS-Ir ₁₀	3a	19
4	APS-Ir ₄₀	3b	59
5	no PC	3a	n.p. ^d
6	C ₂	3a	n.p. ^d

^aSee SI for experimental details. ^bConversion from ^1H NMR. ^cIsolated yield in parentheses. ^dNo product.

by ^1H NMR, which is consistent with literature data,³⁸ resulted in being completely neglected when the complex is not confined within the SCNP (see the SI).

Next, we evaluated the capability of APS-Ir₁₀, APS-Ir₂₃, and APS-Ir₄₀ to catalyze visible-light-induced α -arylation of arylamines that, since its discovery reported by McMillan et al.,^{39,40} have never been reported in water. Table 5, entries 1–3 show the procedure in organic solvents. To enable the photocatalytic cycle to occur in water, we prepared APS-Ir₄₀ by dissolving 2 mg of P1-Ir40 in 1 mL of degassed deionized water. We then charged the APS aqueous solution with 29 μmol of **6** and with a large excess of sodium acetate, NaOAc, (84 equiv). The resulting mixture was deoxygenated by three consecutive vacuum/argon backfill cycles, finally 87 μmol of **5**

Table 5. Photocatalyzed “in Water” α -Arylation of Arylamines (AA Reaction)^a


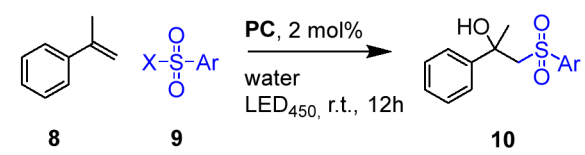
entry	PC	mol % PC	[NaOAc] M ^b	solvent ^b	c% ^c
1	C ₂	0.5	0.06	DMA	>95(95) ^d
2	P ₁ -Ir ₄₀	0.5	0.06	DMA	>95
3	C ₂	0.5	0.06	MeOH	8
4	APS-Ir ₄₀	2	0.06	H ₂ O	n.p. ^e
5	APS-Ir ₄₀	2	2.4	H ₂ O	57(48) ^d
6	APS-Ir ₂₃	2	2.4	H ₂ O	22
7	APS-Ir ₁₀	2	2.4	H ₂ O	21
8	C ₂	2	2.4	H ₂ O	n.p. ^e
9	APS-Ir ₄₀	2	2.4	H ₂ O+DMA	33
10	APS-Ir ₄₀	2	sat. ^f	H ₂ O	24
11	no PC		2.4	H ₂ O	n.p. ^e

^aSee the SI for experimental details. ^bNaOAc = sodium acetate; DMA = dimethylacetamide; MeOH = methanol. ^cConversion of 7 from ¹H NMR. ^dIsolated yield of 7 in parentheses. ^eNo product. ^fSaturated in NaOAc.

were added and left stirring at room temperature and under blue LED ($\lambda_{\max} = 450$ nm) irradiation for 12 h. Under these conditions, product 7 was obtained by using APS-Ir₄₀ as photocatalyst in 57% conversion and 48% purified yield (Table 5, entry 5). Conversion was found to decrease upon reduction of the iridium loading in the APS photocatalyst (Table 5, entries 6 and 7). We attributed the striking conversion drop upon either lowering or increasing the base concentration (Table 5, entries 4 and 10) to the altered acidities of the reactants and additives in aqueous media with respect to the reaction conditions reported in literature for organic solvent.^{39,41}

Inspired by pioneering work by Lipshutz et al.,¹¹ we tested APS-Ir₁₀, APS-Ir₂₃, and APS-Ir₄₀ as photocatalysts for the “in water” β -hydroxysulfonylation of α -methylstyrene 8. We carried out the photocatalytic reactions under oxygen-free conditions by charging the readily prepared APS aqueous solutions with 8 and sulfonyl halides 9 (see the SI). Despite the intrinsic water-sensitive nature of these reactants, we could observe up to 67% conversion into desired product 10 (58% isolated yield) (Table 6, entry 2). As expected, a significant reduction was observed with the model compound C₂ as a photocatalyst (Table 6, entry 6). For this reaction, no significant effect of iridium loading in the APS photocatalyst on conversion is observed (Table 6, entries 1–3).

In summary, artificial photosyntheses (APS) arise by endowing enzyme-mimetic single-chain nanoparticles, SCNPs, with broad visible-light photocatalytic activity for challenging “in water” organic reactions. We introduce a first generation of APS resulting from the decoration of an amphiphilic high-molecular-weight copolymer, poly-(OEGMA₃₀₀-*r*-AEMA), with iridium(III) cyclometalated complex pendants followed by its own self-assembly in water. APS enabled efficient visible-light photocatalysis of a variety of organic transformations in an aqueous solution at room temperature and under LED illumination ($\lambda_{\max} = 450$ nm). This work broadens the possibilities for performing challenging

Table 6. Photocatalyzed “in Water” β -Hydroxysulfonylation of α -Methylstyrene (HS Reaction)^a


entry	PC	transformation	c% ^b
1	APS-Ir ₄₀	9a → 10a	50
2	APS-Ir ₂₃	9a → 10a	67(58) ^d
3	APS-Ir ₁₀	9a → 10a	52
4	APS-Ir ₂₃	9b → 10b	n.p. ^e
5	APS-Ir ₂₃	9c → 10c	21
6	C ₂	9a → 10a	23
7	no PC	9a → 10a	n.p. ^e

^aSee the SI for experimental details. ^bConversion from ¹H NMR. ^dIsolated yield in parentheses. ^eNo product.

“in water” organic transformations via APS-mediated visible-light photocatalysis.

ASSOCIATED CONTENT

Supporting Information

The Supporting Information is available free of charge at <https://pubs.acs.org/doi/10.1021/jacs.4c02718>.

Materials and methods, synthesis and characterization of compounds, effect of APS type on conversion, kinetic assays of APS, recyclability of APS, SEC chromatograms, DLS data, UV–vis spectra, NMR spectra and supplementary references (PDF)

AUTHOR INFORMATION

Corresponding Authors

Davide Arena – Centro de Física de Materiales (CSIC-UPV/EHU)-Materials Physics Center MPC, E-20018 Donostia, Spain; Email: darena001@ikasle.ehu.es

José A. Pomposo – Centro de Física de Materiales (CSIC-UPV/EHU)-Materials Physics Center MPC, E-20018 Donostia, Spain; IKERBASQUE-Basque Foundation for Science, E-48009 Bilbao, Spain; Departamento de Polímeros y Materiales Avanzados: Física, Química y Tecnología, University of the Basque Country (UPV/EHU), Faculty of Chemistry, E-20018 Donostia, Spain; orcid.org/0000-0003-4620-807X; Email: Josetxo.pomposo@ehu.es

Authors

Ester Verde-Sesto – Centro de Física de Materiales (CSIC-UPV/EHU)-Materials Physics Center MPC, E-20018 Donostia, Spain; IKERBASQUE-Basque Foundation for Science, E-48009 Bilbao, Spain; orcid.org/0000-0001-8748-5140

Iván Rivilla – IKERBASQUE-Basque Foundation for Science, E-48009 Bilbao, Spain; Departamento de Química Orgánica I, Centro de Innovación en Química Avanzada (ORFEO-CINQA), University of the Basque Country (UPV/EHU), Faculty of Chemistry, E-20018 Donostia, Spain; Donostia International Physics Center (DIPC), E-

20018 Donostia, Spain; orcid.org/0000-0003-1984-7183

Complete contact information is available at:
<https://pubs.acs.org/10.1021/jacs.4c02718>

Author Contributions

The manuscript was written through contributions of all authors. All authors have given approval to the final version of the manuscript.

Notes

The authors declare no competing financial interest.

ACKNOWLEDGMENTS

We gratefully acknowledge Grant PID2021-123438NB-I00 funded by MCIN/AEI/10.13039/501100011033 and “ERDF A way of making Europe”, Grant TED2021-130107A-I00 funded by MCIN/AEI/10.13039/501100011033 and Unión Europea “NextGenerationEU/PRTR,” and Grant IT-1566-22 from Eusko Jaurlaritz (Basque Government). E.V.-S. acknowledges financial support from RyC program (RYC2022-037590-I). We thank Zoraida Freixa and Ane Aranburu for technical support.

REFERENCES

- (1) Emmanuel, M. A.; Bender, S. G.; Bilodeau, C.; Carceller, J. M.; DeHovitz, J. S.; Fu, H.; Liu, Y.; Nicholls, B. T.; Ouyang, Y.; Page, C. G.; Qiao, T.; Raps, F. C.; Sorigué, D. R.; Sun, S.-Z.; Turek-Herman, J.; Ye, Y.; Rivas-Souchet, A.; Cao, J.; Hyster, T. K. Photobiocatalytic strategies for organic synthesis. *Chem. Rev.* **2023**, *123*, 5459–5520.
- (2) Alphand, V.; Van Berkel, W. J. H.; Jurkaš, V.; Kara, S.; Kourist, R.; Kroutil, W.; Mascia, F.; Nowaczyk, M. M.; Paul, C. E.; Schmidt, S.; Spasic, J.; Tamagnini, P.; Winkler, C. K. Exciting enzymes: Current state and future perspective of photobiocatalysis. *ChemPhotoChem.* **2023**, *7*, No. e202200325.
- (3) Sancar, A. Structure and function of DNA photolyase. *Biochemistry* **1994**, *33*, 2–9.
- (4) Trimble, S. J.; Crawshaw, R.; Hardy, F. J.; Levy, C. W.; Brown, M. J. B.; Fuerst, D. E.; Heyes, D. J.; Obexer, R.; Green, A. P. A designed photoenzyme for enantioselective [2 + 2] cycloadditions. *Nature* **2022**, *611*, 709–714.
- (5) Jeong, W. J.; Lee, J.; Eom, H.; Song, W. J. A specific guide for metalloenzyme designers: introduction and evolution of metal-coordination spheres embedded in protein environments. *Acc. Chem. Res.* **2023**, *56*, 2416–2425.
- (6) Fu, Y.; Huang, J.; Wu, Y.; Liu, X.; Zhong, F.; Wang, J. Biocatalytic cross-coupling of aryl halides with a genetically engineered photosensitizer artificial dehalogenase. *J. Am. Chem. Soc.* **2021**, *143*, 617–622.
- (7) Russo, C.; Brunelli, F.; Tron, C. G.; Giustiniano, M. Visible-light photoredox catalysis in water. *J. Org. Chem.* **2023**, *88*, 6284–6293.
- (8) Sun, K.; Lv, Q.-Y.; Chen, X.-L.; Qu, L.-B.; Yu, B. Recent advances in visible-light-mediated organic transformations in water. *Green Chem.* **2021**, *23*, 232–248.
- (9) Hong, D.; Shi, L.; Liu, X.; Ya, H.; Han, X. Photocatalysis in water-soluble supramolecular metal organic complex. *Molecules* **2023**, *28*, 4068.
- (10) Bottecchia, C.; Noël, T. Photocatalytic modification of amino acids, peptides and proteins. *Chem.—Eur. J.* **2019**, *25*, 26–42.
- (11) Bu, M.-J.; Cai, C.; Gallou, F.; Lipshutz, B. H. PQS-enabled visible-light iridium photoredox catalysis in water at room temperature. *Green Chem.* **2018**, *20*, 1233–1237.
- (12) Mundsinger, K.; Tuten, B. T.; Wang, L.; Neubauer, K.; Kropf, C.; O'Mara, M. L.; Barner-Kowollik, C. Visible-light-reactive single-chain nanoparticles. *Angew. Chem., Int. Ed.* **2023**, *62*, No. e202302995.
- (13) *Single-chain polymer nanoparticles: synthesis, characterization, and applications*; Pomposo, J., Ed.; Wiley-VCH, 2017.
- (14) (a) Rothfuss, H.; Knöfel, N. D.; Roesky, P. W.; Barner-Kowollik, C. Single-chain nanoparticles as catalytic nano-reactors. *J. Am. Chem. Soc.* **2018**, *140*, 5875–5881. (b) Knöfel, N. D.; Rothfuss, H.; Willenbacher, J.; Barner-Kowollik, C.; Roesky, P. W. Platinum (II)-Crosslinked Single-Chain Nanoparticles: An Approach towards Recyclable Homogeneous Catalysts. *Angew. Chem., Int. Ed.* **2017**, *56*, 4950–4954. (c) Liu, Y.; Pujals, S.; Stals, P. J. M.; Paulöhr, T.; Presolski, S. I.; Meijer, E. W.; Albertazzi, L.; Palmans, A. R. A. Catalytically active single-chain polymeric nanoparticles: exploring their functions in complex biological media. *J. Am. Chem. Soc.* **2018**, *140*, 3423–3433.
- (15) Rubio-Cervilla, J.; González, E.; Pomposo, J. A. Advances in single chain nanoparticles for catalysis applications. *Nanomaterials* **2017**, *7*, 341.
- (16) Verde-Sesto, E.; Arbe, A.; Moreno, A. J.; Cangialosi, D.; Alegría, A.; Colmenero, J.; Pomposo, J. A. Single-chain nanoparticles: opportunities provided by internal and external confinement. *Mater. Horiz.* **2020**, *7*, 2292–2313.
- (17) Xiong, T. M.; Garcia, E. S.; Chen, J.; Zhu, L.; Alzona, A. J.; Zimmerman, S. C. Enzyme-like catalysis by single chain nanoparticles that use transition metal cofactors. *Chem. Commun.* **2022**, *58*, 985–988.
- (18) Mundsinger, K.; Izuagbe, A.; Tuten, B. T.; Roesky, P. W.; Barner-Kowollik, C. Single chain nanoparticles in catalysis. *Angew. Chem., Int. Ed.* **2024**, *63*, No. e202311734.
- (19) Chen, R.; Berda, E. 100th Anniversary of macromolecular science viewpoint: re-examining single-chain nanoparticles. *ACS Macro Lett.* **2020**, *9*, 1836–1843.
- (20) (a) Spicuzza, M.; Gaikwad, S. P.; Huss, S.; Lee, A.; Craescu, C. V.; Griggs, A.; Joseph, J.; Puthenpurayil, M.; Lin, W.; Matarazzo, C.; Baldwin, S.; Perez, V.; Rodriguez-Acevedo, D. A.; Swierk, J. R.; Elaqua, E. Visible-Light-Mediated Diels-Alder Reactions Under Single-Chain Polymer Confinement: Investigating the Role of the Crosslinking Moiety on Catalyst Activity. *ChemRxiv*, September 14, 2023, ver. 2. DOI: 10.26434/chemrxiv-2023-zwvsq-v2. (b) Eisenreich, F.; Palmans, A. R. A. Direct C-H Trifluoromethylation of (Hetero)-Arenes in Water Enabled by Organic Photoredox-Active Amphiphilic Nanoparticles. *Chem.—Eur. J.* **2022**, *28*, No. e2022013. (c) Eisenreich, F.; Meijer, E. W.; Palmans, A. R. A. Amphiphilic Polymeric Nanoparticles for Photoredox Catalysis in Water. *Chem.—Eur. J.* **2020**, *26*, 10355–10361.
- (21) Ulbricht, C.; Becer, C. R.; Winter, A.; Schubert, U. S. RAFT polymerization meets coordination chemistry: synthesis of a polymer-based iridium(III) emitter. *Macromol. Rapid Commun.* **2010**, *31*, 827–833.
- (22) Pomposo, J. A.; Colmenero, J.; Kohlbrecher, J.; Arbe, A.; Sanchez-Sanchez, A. Efficient synthesis of single-chain globules mimicking the morphology and polymerase activity of metalloenzymes. *Macromol. Rapid Commun.* **2015**, *36*, 1592–1597.
- (23) Robles-Hernandez, B.; González, E.; Pomposo, J. A.; Colmenero, J.; Alegría, A. Water dynamics and self-assembly of single-chain nanoparticles in concentrated solutions. *Soft Matter* **2020**, *16*, 9738–9745.
- (24) Chen, Z.; Jiang, J.; Zhao, W.; Hu, X.; Xie, M.; Li, F.; Liu, S.; Zhao, Q. An aggregation-induced phosphorescent emission-active iridium(III) complex for fluoride anion imaging in living cells. *J. Organomet. Chem.* **2021**, *932*, 121644.
- (25) Di, L.; Xing, Y.; Yang, Z.; Qiao, C.; Xia, Z. Sens. Photostable aggregation-induced emission of iridium(III) complex realizing robust and high-resolution imaging of latent fingerprints. *Actuators B Chem.* **2023**, *375*, 132898.
- (26) Twilton, J.; Le, C.; Zhang, P.; Shaw, M. H.; Evans, R. W.; MacMillan, D. W. C. The merger of transition metals and photocatalysis. *Nat. Rev. Chem.* **2017**, *1*, 0052.
- (27) Strieth-Kalthoff, F.; James, J. J.; Teders, M.; Pitzer, L.; Glorius, F. Energy transfer catalysis mediated by visible light: principles, applications, directions. *Chem. Soc. Rev.* **2018**, *47*, 7190–7202.
- (28) Shon, J.-H.; Kim, D.; Rathnayake, M. D.; Sittel, S.; Weaver, J.; Teets, T. S. Photoredox catalysis on unactivated substrates with

strongly reducing iridium photosensitizers. *Chem. Sci.* **2021**, *12*, 4069–4078.

(29) (a) Poplata, S.; Tröster, A.; Zou, Y.-Q.; Bach, T. Recent advances in the synthesis of cyclobutanes by olefin [2 + 2] photocycloaddition reactions. *Chem. Rev.* **2016**, *116*, 9748–9815. (b) Du, J.; Yoon, T. P. Crossed intermolecular [2+] cycloadditions of acyclic enones via visible light photocatalysis. *Chem. Soc.* **2009**, *131*, 14604–14605. (c) Pagire, S. K.; Hossain, A.; Traub, L.; Kerres, S.; Reiser, O. Photosensitized regioselective [2 + 2]-cycloaddition of cinnamates and related alkenes. *Chem. Commun.* **2017**, *53*, 12072–12075. (d) Zhao, J.; Brosmer, J. L.; Tang, Q.; Yang, Z.; Houk, K. N.; Diaconescu, P. L.; Kwon, O. Intramolecular crossed [2 + 2] photocycloaddition through visible light-induced energy transfer. *J. Am. Chem. Soc.* **2017**, *139*, 9807–9810. (e) Lu, Z.; Yoon, T. P. Visible light photocatalysis of [2 + 2] styrene cycloadditions by energy transfer. *Angew. Chem., Int. Ed.* **2012**, *51*, 10329–10332. (f) Tanaka, K.; Iwama, Y.; Kishimoto, M.; Ohtsuka, N.; Hoshino, Y.; Honda, K. Redox potential controlled selective oxidation of styrenes for regio- and stereoselective crossed intermolecular [2 + 2] cycloaddition via organophotoredox catalysis. *Org. Lett.* **2020**, *22*, 5207–5211.

(30) Roth, H. G.; Romero, N. A.; Nicewicz, D. A. Experimental and calculated electrochemical potentials of common organic molecules for applications to single-electron redox chemistry. *Synlett* **2016**, *27*, 714–723.

(31) Prier, C. K.; Rankic, D. A.; MacMillan, D. W. C. Visible light photoredox catalysis with transition metal complexes: applications in organic synthesis. *Chem. Rev.* **2013**, *113*, 5322–5363.

(32) (a) Eady, S. C.; MacInnes, M. M.; Lehnert, N. Immobilized cobalt bis(benzenedithiolate) complexes: exceptionally active heterogeneous electrocatalysts for dihydrogen production from mildly acidic aqueous solutions. *Inorg. Chem.* **2017**, *56*, 11654–11667. (b) Naumann, R.; Goez, M. How the Sustainable Solvent Water Unleashes the Photoredox Catalytic Potential of Ruthenium Polypyridyl Complexes for Pinacol Couplings. *Green Chem.* **2019**, *21*, 4470–4474. (c) Glaser, F.; Larsen, C. B.; Kerzig, C.; Wenger, O. S. Aryl Dechlorination and Defluorination with an Organic Super-Photoreductant. *Photochem. Photobiol. Sci.* **2020**, *19*, 1035–1041. (d) Xue, D.; Jia, Z.; Zhao, C.; Zhang, Y.; Wang, C.; Xiao, J. Direct Arylation of N-Heteroarenes with Aryldiazonium Salts by Photoredox Catalysis in Water. *Chem.—Eur. J.* **2014**, *20*, 2960–2965. (e) Vo, N. T.; Mekmouche, Y.; Tron, T.; Guillot, R.; Banse, F.; Halime, Z.; Sircoglou, M.; Leibl, W.; Aukauloo, A. A Reversible Electron Relay to Exclude Sacrificial Electron Donors in the Photocatalytic Oxygen Atom Transfer Reaction with O₂ in Water. *Angew. Chem., Int. Ed.* **2019**, *58*, 16023–16027. (f) Giedyk, M.; Narobe, R.; Weiß, S.; Touraud, D.; Kunz, W.; König, B. Photocatalytic Activation of Alkyl Chlorides by Assembly-Promoted Single Electron Transfer in Microheterogeneous Solutions. *Nat. Catal.* **2020**, *3*, 40–47.

(33) Montalti, M.; Credi, A.; Prodi, L.; Gandolfi, M. T. *Handbook of Photochemistry*; CRC Press: Boca Raton, FL, 2006.

(34) (a) Kawajiri, T.; Kato, M.; Nakata, H.; Goto, R.; Aibara, S.; Ohta, R.; Fujioka, H.; Sajiki, H.; Sawama, Y. Aromatic aldehydes and acetals via pyridinium salt intermediates. *J. Org. Chem.* **2019**, *84*, 3853–3870. (b) Christensen, S. H.; Olsen, E. P. K.; Rosenbaum, J.; Madsen, R. Hydroformylation of olefins and reductive carbonylation of aryl halides with syngas formed ex situ from dehydrogenative decarbonylation of hexane-1,6-diol. *Org. Biomol. Chem.* **2015**, *13*, 938–945. (c) Despras, G.; Zamaleeva, A. I.; Dardevet, L.; Tisseyre, C.; Magalhaes, J. G.; Garner, C.; De Waard, M.; Amigorena, S.; Feltz, A.; Mallet, J.-M.; Collot, M. H-Rubies, a new family of red emitting fluorescent pH sensors for living cells. *Chem. Sci.* **2015**, *6*, 5928–5937. (d) Schmidt, B.; Elizarov, N.; Berger, R.; Holter, F. Scope and limitation of the Heck-Matsuda-coupling of phenol diazonium salts and styrenes: a protecting-group economic synthesis of phenolic stilbenes. *Org. Biomol. Chem.* **2013**, *11*, 3674–3691. (e) Hussain, M. I.; Feng, Y.; Hu, L.; Deng, Q.; Zhang, X.; Xiong, Y. Copper-catalyzed oxidative difunctionalization of terminal unactivated alkenes. *J. Org. Chem.* **2018**, *83*, 7852–7859. (f) Murphy-Benvenuto, K. E.; Olivier, N.; Choy, A.; Ross, P. L.; Miller, M. D.; Thresher, J.; Gao, N.; Hale, M. R.

Synthesis, structure, and SAR of tetrahydropyran-based LpxC inhibitors. *ACS Med. Chem. Lett.* **2014**, *5*, 1213–1218.

(35) (a) Naik, A.; Meina, L.; Zabel, M.; Reiser, O. Efficient aerobic Wacker oxidation of styrenes using palladium bis(isonitrile) catalysts. *Chem.—Eur. J.* **2010**, *16*, 1624–1628. (b) Daw, P.; Petakamsetty, R.; Sarbajna, A.; Laha, S.; Ramapanicker, R.; Bera, J. K. A highly efficient catalyst for selective oxidative scission of olefins to aldehydes: abnormal-NHC-Ru(II) complex in oxidation chemistry. *J. Am. Chem. Soc.* **2014**, *136* (40), 13987–13990. (c) Xu, J.; Zhang, Y.; Yue, X.; Huo, J.; Xiong, D.; Zhang, P. Selective oxidation of alkenes to carbonyls under mild conditions. *Green Chem.* **2021**, *23*, 5549–5555.

(36) (a) Gao, R.; Ho, D. G.; Hernandez, B.; Selke, M.; Murphy, D.; Djurovich, P. I.; Thompson, M. E. Bis-cyclometalated Ir(III) complexes as efficient singlet oxygen sensitizers. *J. Am. Chem. Soc.* **2002**, *124*, 14828–14829. (b) Xu, Y.; Wang, X.; Song, K.; Du, J.; Liu, J.; Miao, Y.; Li, Y. BSA-encapsulated cyclometalated iridium complexes as nano-photosensitizers for photodynamic therapy of tumor cells. *RSC Adv.* **2021**, *11*, 15323–15331. (c) Jiang, X.; Peng, J.; Wang, J.; Guo, X.; Zhao, D.; Ma, Y. Iridium-based high-sensitivity oxygen sensors and photosensitizers with ultralong triplet lifetimes. *ACS Appl. Mater. Interfaces* **2016**, *8*, 3591–3600. (d) Ashen-Garry, D.; Selke, M. Singlet oxygen generation by cyclometalated complexes and applications. *Photochem. Photobiol.* **2014**, *90*, 257–274. (e) McKenzie, L. K.; Sazanovich, I. V.; Baggaley, E.; Bonneau, M.; Guerschais, V.; Williams, J. A. G.; Weinstein, J. A.; Bryant, H. E. Metal complexes for two-photon photodynamic therapy: a cyclometalated iridium complex induces two-photon photosensitization of cancer cells under near-IR light. *Chem.—Eur. J.* **2017**, *23*, 234–238. (f) Xu, Y.; Wang, X.; Song, K.; Du, J.; Liu, J.; Miao, Y.; Li, Y. BSA-encapsulated cyclometalated iridium complexes as nano-photosensitizers for photodynamic therapy of tumor cells. *RSC Adv.* **2021**, *11*, 15323–15331. (g) Maggioni, D.; Galli, M.; D'Alfonso, L.; Inverso, D.; Dozzi, M. V.; Sironi, L.; Iannaccone, M.; Collini, M.; Ferruti, P.; Ranucci, E.; D'Alfonso, G. A luminescent poly(amidoamine)-iridium complex as new singlet-oxygen sensitizer for photodynamic therapy. *Inorg. Chem.* **2015**, *54*, 544–553. (h) Qin, W.-W.; Pan, Z.-Y.; Cai, D.-H.; Li, Y.; He, L. Cyclometalated iridium(III)-complexes for mitochondria-targeted combined chemo-photodynamic therapy. *Dalton Trans.* **2020**, *49*, 3562. (i) Zamora, A.; Viguera, G.; Rodríguez, V.; Santana, M. D.; Ruiz, J. Cyclometalated iridium(III) luminescent complexes in therapy and phototherapy. *Coord. Chem. Rev.* **2018**, *360*, 34–76.

(37) (a) Zhao, J.-L.; Jiang, X.-K.; Wu, C.; Wang, C.-Z.; Zeng, X.; Redshaw, C.; Yamato, T. An unprecedented photochemical reaction for anthracene-containing derivatives. *ChemPhysChem* **2016**, *17*, 3217–3222. (b) Jacob, J. P.; Gopalakrishnan, R.; Mallia, R. R.; Vadakkan, J. J.; Unnikrishnan, P. A.; Prathapan, S. Dramatic solvent and concentration dependence in the reaction of (anthracen-9-yl)methanamines with suitable electron-deficient acetylenes. *Phys. Org. Chem.* **2014**, *27*, 884–891. (c) Adam, W.; Prein, M. Diastereoselective [4 + 2] cycloaddition of singlet oxygen in the photooxygenation of chiral naphthyl alcohols: evidence for a hydroxy group-directing effect. *J. Am. Chem. Soc.* **1993**, *115*, 3766–3767. (d) Mondal, S.; Mondal, S.; Midya, S. P.; Das, S.; Mondal, S.; Ghosh, P. Merging photocatalytic C-O cross-coupling for α -oxycarbonyl- β -ketones: esterification of carboxylic acids via a decarboxylative pathway. *Org. Lett.* **2023**, *25*, 184–189.

(38) (a) Natarajan, P.; Vagicherla, V. D.; Vijayan, M. T. A mild oxidation of deactivated naphthalenes and anthracenes to corresponding para-quinones by N-bromosuccinimide. *Tetrahedron Lett.* **2014**, *55*, 3511–3515. (b) Pankhurst, J. R.; Curcio, M.; Sproules, S.; Lloyd-Jones, G. C.; Love, J. B. Earth-abundant mixed-metal catalysts for hydrocarbon oxygenation. *Inorg. Chem.* **2018**, *57*, 5915–5298. (c) Chatani, N.; Kamitani, A.; Oshita, M.; Fukumoto, Y.; Murai, S. Catalytic carbonylation reactions of benzene derivatives. *J. Am. Chem. Soc.* **2001**, *123*, 12686–12687. (d) Majumdar, B.; Bhattacharya, T.; Sarma, T. K. Gold nanoparticle-polydopamine-reduced graphene oxide ternary nanocomposite as efficient catalyst for selective oxidation of benzylic C(sp³)-H bonds under mild conditions. *ChemCatChem.* **2016**, *8* (10), 1825–1835. (e) Dong, C.-P.;

Higashiura, Y.; Marui, K.; Kumazawa, S.; Nomoto, A.; Ueshima, M.; Ogawa, A. Metal-free oxidative coupling of benzylamines to imines under an oxygen atmosphere promoted using salicylic acid derivatives as organocatalysts. *ACS Omega* **2016**, *1*, 799–807.

(39) McNally, A.; Prier, C. K.; MacMillan, D. W. C. Discovery of an α -amino C-H arylation reaction using the strategy of accelerated serendipity. *Science* **2011**, *334*, 1114–1117.

(40) Prier, C. K.; MacMillan, D. W. C. Amine α -heteroarylation via photoredox catalysis: a homolytic aromatic substitution pathway. *Chem. Sci.* **2014**, *5*, 4173–4178.

(41) (a) Zhang, X.; Yeh, S.-R.; Hong, S.; Freccero, M.; Albini, A.; Falvey, D. E.; Mariano, P. S. Dynamics of α -CH deprotonation and α -desilylation reactions of tertiary amine cation radicals. *J. Am. Chem. Soc.* **1994**, *116*, 4211–4220. (b) Yoon, U. C.; Mariano, P. S. Mechanistic and synthetic aspects of amine-enone single electron transfer photochemistry. *Acc. Chem. Res.* **1992**, *25*, 233–240. (c) Eckert, F.; Leito, I.; Kaljurand, I.; Kütt, A.; Klamt, A.; Diedenhofen, M. Prediction of acidity in acetonitrile solution with COSMO-RS. *J. Comput. Chem.* **2009**, *30*, 799–810.